

รายงานวิจัยฉบับสมบูรณ์

โครงการ การออกแบบโพรบสำหรับทำลายเนื้อเยื่อโดยความร้อนแบบไมโครเวฟ เพื่อรักษาโรคมะเร็งและการศึกษาเปรียบเทียบถึงประสิทธิภาพของโพรบแบบคลื่น ความถี่วิทยุและแบบไมโครเวฟ

> DESIGN OF MICROWAVE ABLATION PROBES FOR CANCER TREATMENT AND A COMPARATIVE STUDY OF RADIO-FREQUENCY AND MICROWAVE ABLATION

> > โดย ผศ.ดร. สุพันธุ์ ตั้งจิตกุศลมั่น

สัญญาเลขที่ TRG4580106

รายงานวิจัยฉบับสมบูรณ์

โครงการ การออกแบบโพรบสำหรับทำลายเนื้อเยื่อโดยความร้อนแบบไมโครเวฟ เพื่อรักษา โรคมะเร็งและการศึกษาเปรียบเทียบถึงประสิทธิภาพของโพรบแบบคลื่นความถี่วิทยุและ แบบไมโครเวฟ

> DESIGN OF MICROWAVE ABLATION PROBES FOR CANCER TREATMENT AND A COMPARATIVE STUDY OF RADIO-FREQUENCY AND MICROWAVE ABLATION

โดย ผศ.ดร. สุพันธุ์ ตั้งจิตกุศลมั่น
ภาควิชาอิเล็กทรอนิกส์
คณะวิศวกรรมศาสตร์
สถาบันเทคโนโลยีพระจอมเกล้าเจ้าคุณทหารลาดกระบัง

สนับสนุนโดยสำนักงานกองทุนสนับสนุนการวิจัย

(ความเห็นในรายงานนี้เป็นของผู้วิจัย สกว.ไม่จำเป็นต้องเห็นด้วยเสมอไป)

กิตติกรรมประกาศ

ผู้วิจัยขอขอบพระคุณสำนักบริการคอมพิวเตอร์ สถาบันเทคโนโลยีพระจอมเกล้าเจ้าคุณทหาร ลาดกระบังที่ให้การสนับสนุนอุปกรณ์และซอฟท์แวร์ในการทำงานวิจัย และขอขอบพระคุณ Prof. John G. Webster และ James A. Will University of Wisconsin-Madison ที่ให้คำแนะนำปรึกษาต่างๆ ตลอดมา

บทคัดย่อ

รหัสโครงการ: TRG4580106

ชื่อโครงการ: การออกแบบโพรบสำหรับทำลายเนื้อเยื่อโดยความร้อนแบบไมโครเวฟเพื่อรักษา

โรคมะเร็งและการศึกษาเปรียบเทียบถึงประสิทธิภาพของโพรบแบบคลื่นความถึ่

วิทยุและแบบไมโครเวฟ

ชื่อนักวิจัย: สุพันธุ์ ตั้งจิตกุศลมั่น

ภาควิชาอิเล็กทรอนิกส์ คณะวิศวกรรมศาสตร์

สถาบันเทคโนโลยีพระจอมเกล้าเจ้าคุณทหารลาดกระบัง

Email Address: ktsupan@gmail.com

ระยะเวลาโครงการ: 1 ก.ค. 2545 ถึงวันที่ 31 ธ.ค. 2551

โรคมะเร็งเป็นสาเหตุของการเสียชีวิตของผู้คนในโลกเป็นจำนวนนับล้านคนต่อปี ทำได้โดยการผ่าตัดเพื่อเฉือนเอาก้อนเนื้อมะเร็งออก โดยทั่วไปนั้น ซึ่งทำให้เกิดการเสียเลือด ปริมาณมาก และมักไม่เหมาะสมกับผู้ป่วย ได้มีการนำเสนอวิธีการรักษามะเร็งในเนื้อเยื่อตับอื่นๆ เช่น การฉีดสารเคมี หรือ วิธีการ Cryosurgery (การทำลายเซลล์มะเร็งด้วยความเย็น) ซึ่งล้วนมี ผลข้างเคียง เช่นมีการเสียเลือดในปริมาณมากและอาจเสี่ยงต่อการติดเชื้อได้ อีกทางเลือกในการ รักษาคือการใช้ความร้อนจากแหล่งกำเนิดทางไฟฟ้าในช่วงคลื่นความถี่วิทยุในการทำลาย เซลล์มะเร็ง ซึ่งก็คือวิธี Radio-frequency (RF) Ablation โดยใช้กระแสไฟฟ้าช่วงคลื่นความถึ่ ประมาณ 500kHz โดยการรักษากระทำผ่านทางผิวหนังและใช้เข็มเป็นตัวเจาะเข้าไปยังเซลล์มะเร็ง ส่วนของปลายเข็มจะเกิดความร้อน การใช้คลื่นความถี่วิทยุมีข้อจำกัดในด้านของขนาดเซลล์มะเร็งที่ ถูกทำลาย จึงมีการวิจัยเพิ่มเติมโดยใช้คลื่นความถี่ไมโครเวฟ (MW) ซึ่งมีความถี่สูง (2.45 GHz) ผ่านสายอากาศที่เสียบอยู่ในเซลล์เนื้อเยื่อที่เป็นมะเร็ง แบบแผนของการกระจายพลังงานแบบ MW นั้น สามารถถูกบังคับควบคุมได้มากกว่าการใช้ RF และอาจสามารถทำลายเซลล์ได้ในบริเวณที่ กว้างกว่าหรือว่ามีลักษณะของกลุ่มเซลล์ที่ถูกทำลายเป็นไปตามที่ต้องการได้ ในงานวิจัยนี้ ได้ทำ การทดลองการใช้ MW ในการทำลายเนื้อเยื่อ โดยใช้สายอากาศพร้อมกัน 3 ต้น รวมทั้งศึกษาถึง การจัดวางสามแบบแผน คือ แบบขนาน แบบสามเหลี่ยม และแบบตั้งฉาก โดยใช้วิธีการไฟในต์เอลิ เมนต์พร้อมกับการทดลองจริงในห้องทดลอง จากผลการทดลองที่ได้นั้น พบว่าการวางสายอากาศ แบบตั้งฉากนั้น สามารถทำลายเนื้อเยื่อได้ปริมาณมากที่สุด โดยมีขนาดความกว้างและความลึกของ การทำลายประมาณ 40 มม. และ 85 มม. ตามลำดับ และปริมาตรเท่ากับ 30.2 ซม³ นอกจากนี้การ ใช้สายอากาศที่มีการออกแบบต่างกันพร้อมๆกันจะทำให้ได้บริเวณการทำลายที่มีลักษณะต่างกัน

Keywords: microwave ablation, finite element analysis, hepatic ablation, bio-heat equation, triple-antenna

Abstract

Project Code: TRG4580106

Project Title: Design of microwave ablation probes for cancer treatment and a

comparative study of radio-frequency and microwave ablation

Investigator: Supan Tungjitkusolmun

Dept. of Electronics, Faculty of Engineering

King Mongkut's Institute of Technology Ladkrabang

Email Address: ktsupan@gmail.com

Project Period: July 1, 2002 to December 31, 2008

Hepatic cancer is one of the leading causes of death of people around the world. Possible treatments for hepatic cancers are surgical operation, chemical treatment, cryoablation, radiation therapy, and radio-frequency (RF) ablation. Currently, surgical resection is the treatment of choice for both well-localized primary and metastatic hepatic malignancies. However, the majority of the patients are not candidates for surgical resection due to certain restrictions. Radio-frequency (RF) ablation has been recently introduced and has proved to be an effective cure for primary hepatic cancer where the tumors found are still small (< 3 cm in diameter. Microwave (MW) ablation method offer a potentially superior method for curing cancer as MW ablation results in a much larger zone of active heating than RF ablation. This study presents analyses of triple-antenna configurations and designs for microwave hepatic ablation. Using multiple antennas offers a potential solution for creating lesions with larger dimensions as well as varied geometrical shapes. We performed both three-dimensional finite element analyses and in vitro experiments using three identical open-tip microwave antennas simultaneously, placing them in three types of configurations—"array", "triangular", and "orthogonal" arrangements. The results illustrate that arranging antennas in the "orthogonal" pattern destroyed more unwanted tissues than those found when using "array" and "triangular" arrangements, with maximum lesion width and depth of 45 mm, and 80 mm, respectively, and lesion volume of 30.2 Cm³. In addition, using non-identical triple-antennas caused variations in lesion characteristics.

Keywords: microwave ablation, finite element analysis, hepatic ablation, bio-heat equation, triple-antenna

<u>1. วัตถุประสงค์</u>

- 1.1 Create a finite element method (FEM) computer model for MW ablation that will predict overall unit performance. We will perform parametric studies of the effects that influence the extent of lesion formation, such as blood flow, specific absorption rate (SAR), temperature setting, power, and application duration.
- 1.2 Construct a simplified MW probe and test several vital parameters include ablation time, required energy, extent of the lesion formed, etc. We will perform ex vivo experiments using bovine and swine tissues.
- 1.3 Design new MW probe designs using FEM and ex vivo experiments

2. ที่มาของงานวิจัย

Hepatic cancer is one of the leading causes of death, especially in Southeast Asia [1]. Two types of hepatic cancer are commonly found—primary and metastatic malignancies. Primary hepatic cancer can potentially be cured if it is discovered in early stages while metastatic hepatic cancer can rarely be treated. Possible treatments for primary hepatic cancers are surgical operation, chemical treatment, cryoablation, radiation therapy, and radio-frequency (RF) ablation [2]. Currently, surgical resection is the treatment of choice for both well-localized primary and metastatic hepatic malignancies [3]. However, the majority of the patients are not candidates for surgical resection due to restrictions, such as multifocal disease, tumor size, location of tumor to key vessels, or coagulopathies. Chemical treatment, where adequate chemical injection is administered into artery supplying cancer tissues, and radiation therapy are mostly used to temporarily relieve the symptoms [2]. A combination of the above methods has also been used for treatment of hepatic cancer to improve the degree of success [4].

RF ablation has been recently introduced and has proved to be an effective cure for primary hepatic cancer where the tumors found are still small (< 3 cm in diameter) [2], [5]—[7]. In RF ablation, electric current at frequencies between 350—500 kHz is passed into cancer cells via an electrode placed inside the tumor. The electric energy generates Joule heat which then conducts into surrounding tissues. Elevating temperature of unwanted tissues to a level above 50 °C can effectively kill cancer cells [8], [9]. RF ablation is much less invasive compared to surgical resection as only a small incision is required for

insertion of ultrasound-guided RF probe. Thus RF ablation reduces risks of side effects and requires less recovery period for patients.

Commonly reported disadvantages in RF ablation technique include difficulty in treating large tumors—that is, those exceeding 3 cm in diameter [10]; the potential for incomplete RF tumor ablation near blood vessels because of the heat sink effect of local blood flow [11], [12], difficulty in obtaining sonographic images of RF lesions; and evidence of surviving tumor cells, even within RF lesions [2], [6]. Treatment of large tumors by performing sequential RF ablations can be time consuming to adequately ensure total overlapping coverage of the ablation zones [2], [7], [13]. Proposed modifications of the conventional RF ablation technique to increase lesion dimensions include injecting cool saline at the distal end of the probes to reduce overheating at regions in close proximity to avoid a sudden increase in impedance, using multiple tines which can increase effective heating area, and the use of multiple RF probes to achieve larger coagulation volumes than those possible with a single probe [14]—[17].

Microwave (MW) ablation method is another alternative for curing cancer and is emerging as a new treatment option for patients with unresectable hepatic malignancies [13], [18]. Similar to RF ablation, MW current is passed to cancer tissues typically via an antenna which causes generation of Joule heat to selective targeted areas. However, the zone of active tissue heating from RF probe is limited to a few millimeters surrounding the active electrode, with the remainder of the ablation zone being heated via thermal conduction [2]. Owing to the much broader field of power density of the electromagnetic field in MW ablation (up to 2 cm surrounding the antenna [2], [7]), MW ablation results in a much larger zone of active heating than RF ablation. In addition, manipulating the designs of MW antenna has a greater effect on electromagnetic field distributions which in turn govern the temperature distributions found in unwanted tissue. RF ablation is also limited by the increase in impedance with tissue boiling and charring because water vapor and char act as electric insulators. Due to the electromagnetic nature of MW, ablations performed do not seem to be subjected to this limitation, thus allowing the intramural temperature to be driven considerably higher, resulting in a larger ablation zone within a shorter ablation duration [2], [7]. Thus, MW ablation offers many of the benefits of RF ablation but has several theoretical advantages that may result in larger lesion formation, and improved performance near blood vessels [2].

Several studies on MW ablation have been previously reported over the past decade. In 1996, Labonté et al. [19] introduced three types of MW antennas—open-tip monopole (OTM), dielectric-tip monopole (DTM), and metal-tip monopole (MTM)—operating at 2.45 GHz for cardiac ablation. They compared the three antenna designs using finite element (FE) analysis and found that MTM provided the smoothest temperature distribution in surrounding tissue. MTM was also found to be well matched at low frequencies but has a high S₁₁ of -5 dB at 2.45 GHz. OTM exhibited the lowest S₁₁ (good matching impedance) at 2.45 GHz and its temperature distribution was found to be relatively smooth.

Saito et al. 2000 [20] used the "MW coagulation therapy (MCT)" system operating at 2.45 GHz with two slot antennas. The antennas were placed in parallel ("array" arrangement) and the power supply was set to 50 W for duration of 90 s, with an optimal distance between the antennas of 10 mm. They simulated with the Finite Different Time Domain (FDTD) method and verified the simulation results with *in vitro* experiment using porcine liver. From the experimental results, the largest lesion width found was approximately 3 cm.

The clinically used MW devices show varying sizes of coagulation volume depending on their geometry: applicators of straight geometry are reported to achieve coagulation diameters of up to 2.5 cm [21], whereas single loop-antenna applicators were reported to result in coagulation diameters of up to 3.5 cm [22]. Other notable proposed MW antenna designs include: cap-choke catheter antenna proposed by Lin et al. [23] for MW treatment with localized heating of tissue surrounding the distal end of the catheter, the floating sleeve antenna proposed by Yang et al. [24] where the inclusion of the floating sleeve could prevent the flow of electromagnetic energy along the coaxial applicator.

Using multiple MW antennas has also been reported to give noticeably larger lesion formations. In addition to double slot-antennas reported by Saito et al. 2000 [20[, Wright et al. 2003 reported that using triple-antenna ablation in a triangular array in *in vivo* experiments produced synergistically larger ablation lesions than those produced by single antenna ablation, thus hinting at the more convenient and effective treatment of large tumors using MW ablation [21]. Additionally, simultaneous triple-antenna ablation results in qualitatively better lesions, with more uniform coagulation and better performance near

blood vessels. Thus, this study will further investigate triple-antenna MW ablation by varying the arrangements of the antennas.

Numerical simulation has been used extensively in studies of RF & MW ablation as it offers a fast and economical way to evaluate new hypothetical designs. Simulations of three-dimensional (3-D) coupled thermal-electric FE analysis were previously introduced for RF ablation [25]—[30]. However all previous FE analysis for MW hepatic ablation have been performed in two dimensions (approximating the geometry of the FE model to be axisymmetric) [20], [23], [24], [31]—[36]. In this study, we performed 3-D FE analyses of triple-antenna MW ablation (at 2.45 GHz) as well as *in vitro* experiments using swine liver tissue. Three antenna designs—open-tip, slot, and slot with insulating jacket—were initially investigated for use in single antenna ablation (Fig. 1). We then introduced three types of triple-antenna arrangements—"array", "triangular", and "orthogonal" patterns—by placing three identical antennas at 10 mm apart in each arrangement configuration. The resulted temperature distributions were compared after application of 50 W for 60 s. We also tested triple-antenna arrangements using three non-identical antenna designs in order to explore the influence of antenna design on temperature distribution of triple-antenna ablation.

3. วิธีทดลอง

In this study, we first compared the heating characteristics of three single antenna designs—"open-tip", "slot", and "slot with insulating jacket", after applying power of 50 W for a duration of 60 s. The structures of these antennas are described in the next section. The antenna design with the largest lesion formation was then selected for use in the comparison of (identical) triple-antenna configurations—"parallel", "triangular", and "orthogonal" patterns. Lastly, we performed triple-antenna MW ablation using three non-identical antenna designs simultaneously ("mixed" triple-antenna) in order to further explore more possibilities for varied lesion characteristics.

TABLE 1

DIMENSIONS OF COMPONENTS OF COAXIAL ANTENNAS

	Dimensions (mm)			
Component	COA	CSA	CIA	
Inner conductor	0.912	0.912	0.912	
Diameter of outer conductor	3.581	3.581	3.581	
Diameter of dielectric	2.985	2.985	2.985	
Width of slot	-	3	3	
Length from end to slot	-	20	20	
Length of open-tip end	20	-	-	
Thickness of outer insulator	-	-	1	
Overall length of antenna	60	60	60	

A. Antenna Designs

The antennas used in the experiment were semi-rigid coaxial cable (RG 402 M17/130-RG402 Copper Jacket, EMC Technology & Florida RF Labs, Stuart, Florida, USA) having a diameter of 3.581 mm, and were used with N-type connector. We modified this semi-rigid coaxial antenna to obtain different antenna designs investigated in this study, which were:

- (1) Coaxial Open-tip Antenna (COA): the outer conductor was stripped off from the distal end of the antenna (20 mm in length) (Fig. 1 (a)).
- (2) Coaxial-slot Antenna (CSA): a 3-mm slot centered at 20 mm from the distal end of the coaxial antenna was cut open (Fig. 1 (b)).
- (3) Coaxial-slot Antenna with Insulator (CIA): a 3-mm slot was cut open at the same fashion as in (2). Similar to Saito et al. 2000 [20], we then covered the slot with polytetrafluoroethylene (PTFE, Shenzhen Woer Heat-Shrinkable Material Co., Ltd., Shenzhen, China), as shown in Fig. 1 (c).

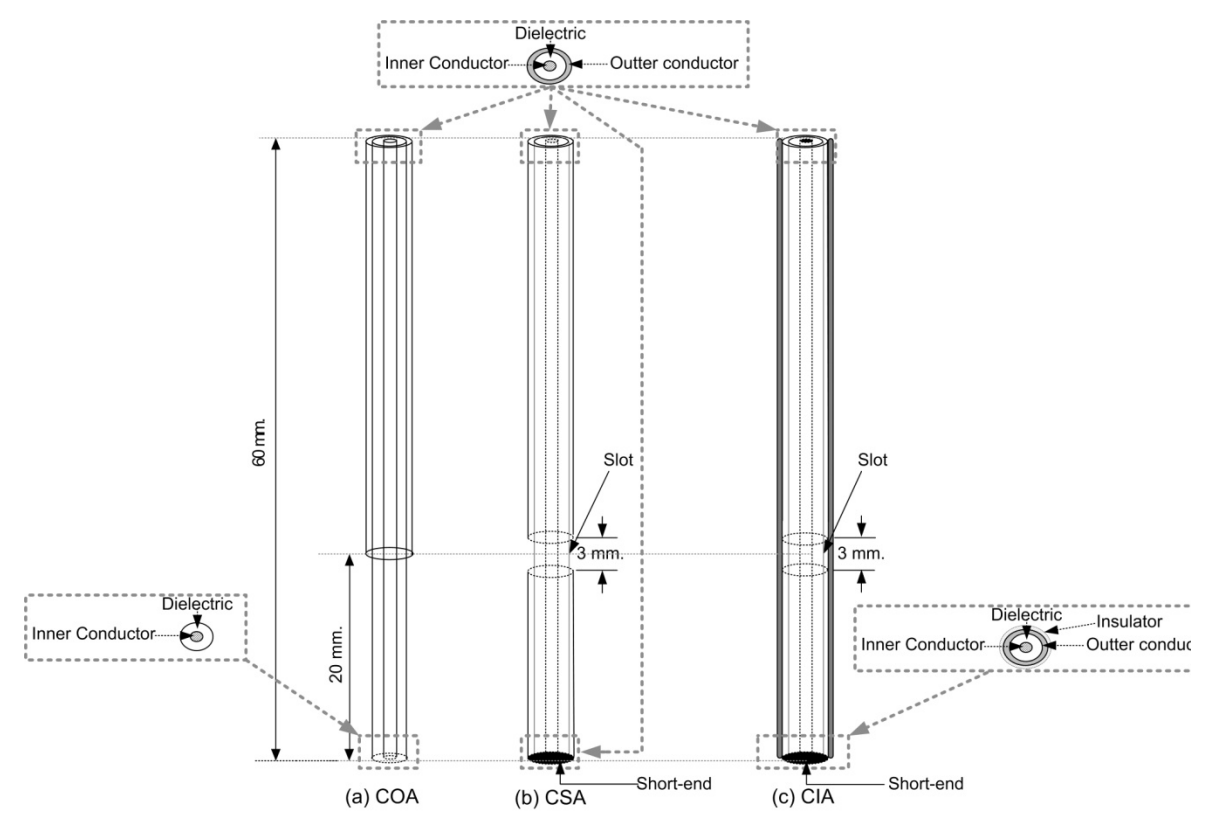


Fig. 1. Structure of Antenna (a) COA (b) CSA and (c) CIA. For COA, the 20 mm distal end of the antenna was stripped off, while a 3-mm slot was cut open for CSA, and CIA. CIA has a 1-mm thick insulating jacket covering the antenna.

Dimensions of the components of these antennas are listed in Table 1. Table 2 lists the material properties of each component of the antennas [37]. These dimensions and properties were incorporated in all FE models in this study.

B. Properties of Antennas

The graphical illustration in Fig. 2 shows properties measured from the Bird Site Analyzer Model SA-6000 EX (Bird Electronic Corporation, Cleveland, Ohio, USA.). We measured Voltage Standing Wave Ratio (VSWR) values of the antennas in the range of 2.3 GHz to 2.6 GHz which covered our operating frequency of 2.45GHz. All measurements were performed by inserting each antenna in a 10 cm x 10 cm excised swine liver. From the results in Fig. 2, all three antenna designs have very low VSWR (1.065, 1.030, and 1.015 for COA, CSA, and CIA, respectively). Antennas with very low VSWR are desirable because they can drive more energy into tissue. Thus, all three antenna designs can potentially be used in MW ablation applications. Note that VSWR of CIA is lower than that

of CSA at all frequencies which indicates that the matching impedance of CIA is better than that of CSA.

TABLE 2
MATERIAL PROPERTIES USED IN FE MODELS [37].

Properties	Value		
$ ho_{liver}$ = Density of liver	1,050 [kg/m³]		
$c_{\it liver}$ = Specific heat of liver	3,700 [<i>J/ kg.K</i>]		
$ ho_{bl}$ = Density of blood	1,000 [<i>kg/ m</i> ³]		
$c_{\it bl}$ = Specific heat of blood	3,639 [J/ kg.K]		
w_{bl} = Blood perfusion rate	$3.6 \times 10^{-3} [m^3/kg.s]$		
k = Thermal conductivity of liver	0.56 [S/m]		
σ_{liver} = electrical conductivity of liver ¹	1.69 [S/m]		
ε_{liver} = relative permittivity of liver ¹	43.03		
$arepsilon_{ m diel}$ = relative permittivity of dielectric	2.03		
$\varepsilon_{\scriptscriptstyle insul}$ = relative permittivity of insulator	2.6		

¹ [Online]. Available: http://niremf.ifac.cnr.it/tissprop/

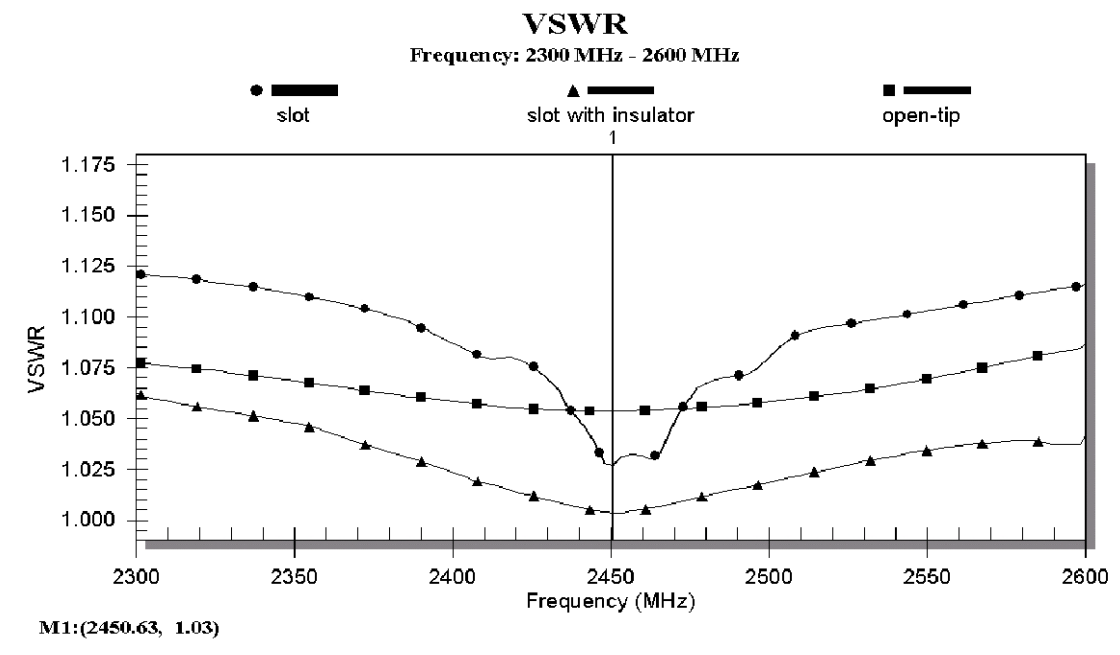


Fig. 2. VSWR characteristics of COA, CSA, and CIA antennas over frequency range of 2300 to 2600 MHz

C. Bio-heat Equation and FEM

The source of heat transfer in MW ablation is from electromagnetic wave at 2.45 GHz transmitted into tissues. Joule heating arises when energy dissipated by an electric current flowing through a conductor is converted into thermal energy. Tissue temperature changes over time can be predicted by the bio-heat equation [38]:

$$\rho C \frac{\partial T}{\partial t} + \nabla \cdot (-k \nabla T) = \rho_b C_b \omega_b (T_b - T) + Q_{met} + Q_{ext}$$
 (1)

where
$$Q_{ext} = \rho.SAR$$
 (2)

$$\mathit{SAR} = \frac{\sigma}{\rho} E^2 \qquad [W/kg]$$
 and

Table 2 lists definitions of parameters and variables in Eq. [1]—[3]. The energy generated by metabolic process (Q_{met}) was neglected in this study since it was small compared to other heat sources [26], [29]. Q_{ext} is external heat source generated by MW energy from antennas. After delivery of MW energy into tissue, Joule heat is generated which then conducts into surrounding tissues. Convective cooling from blood flow in blood vessels of the liver takes away a certain amount of heat from hepatic tissue.

As the geometries of the antennas used in this study were complicated, we utilized mathematical modeling to solve 3-D bio-heat equation in order to obtain temperature distributions during MW ablation. FE Modeling is a powerful tool for solving sophisticated differential equations by dividing domains of interest into small regions, called elements. Thus, complicated differential equations can be simplified into a set of algebraic equations. In this study, we employed the 3-D FE method using COMSOL Multiphysics Version 3.4 (COMSOL Inc., Burlington, MA) on a 64-bit Sun Fire V40z Server (2 processors, 8 GB of RAM). The simulations performed in COMSOL consisted of RF Module and Heat Transfer (Bioheat Equation) Module. We developed the antenna structure and other geometrical components with SolidWorks Version 2007 (SolidWorks Corp, Concord, MA) before exporting them in IGES format into COMSOL Multiphysics 3.4. We assigned boundary conditions and material properties and then solved the coupled thermal-electromagnetic problem. The total time for MW energy application was set to 60 s while the power delivered was set to 50 W for all cases.

TABLE 3. NUMBERS OF ELEMENTS FOR EACH FE MODELS

Configuration	(elements)
Single COA	27,394
Single CSA	30,451
Single CIA	50,096
Array COA	60,420
Triangular COA	71,789
Orthogonal COA	74,283
Array (CSA+COA+CIA)	78,295
Triangular (CSA+COA+CIA)	85,337
Orthogonal (CSA+COA+CIA)	92,037

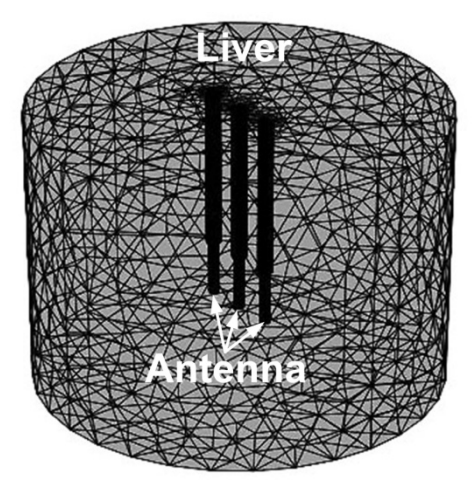


Fig. 3. A typical finite element model used in this study consisting of non-uniform mesh. The case shown above is aray COA.

Fig. 3 shows a non-uniformly meshed 3-D FE model consisting of three antennas placed in an array pattern within hepatic tissue. The mesh used in our models was finer at areas surrounding the distal end of antennas and was coarser at locations further away from the tip of the antennas. The numbers of elements for our three antennas arrangements were approximately 70,000 elements (Table 3) and the numbers of degrees of freedom were in the order of 600,000.

D. Comparison of COA, CSA, and CIA

Before processing to triple-antenna hepatic MW ablation, we first analyzed the characteristics of lesions formed using three different single antenna designs. The structure of COA, CSA, and CIA are shown in Fig. 1. We measured VSWR characteristics of the three single antennas and results are shown in Fig. 2. We then performed FE analyses to compare lesion formations by applying 50 W to each antenna for 60 s and measured areas with temperature exceeding 60 °C (where tissue discoloration occurs [20]).

E. Triple-antenna Configurations

We used the optimal antenna design from section III (d) for triple-antenna MW ablation. To study the effect of antenna arrangements and designs, we performed the FE analyses for the following cases:

- 1) Array Configuration (array): Three identical antennas A, B, and C, were all placed on the y-z plane (x=0) in parallel (Fig. 4 (a)). The distance between two adjacent antennas was 10 mm. The insertion depth of each antenna was 60 mm. The overall geometry of this case was cylindrical with 100 mm in diameter and 80 mm in height. Temperature distributions on y-z plane at x = 0, on x-y plane at z = 0, and z = 00 mm were recorded.
- 2) Triangular Configuration (triangular): Three COA antennas (A, B, and C) were arranged in a three probe cluster-like configuration parallel to the centrally located z-axis, forming an equilateral triangle on the cross-sectional plane (Fig. 4 (b)). The spacing distances between the distal end of antenna A and B, B and C, and A and C were 10 mm. The insertion depth of all antennas was 60 mm. Similar to Case 1, the overall geometry of Case 2 was cylindrical with 100 mm diameter and 80 mm height, and temperature distributions on x-y plane at z=0 and -20 mm were recorded. In addition, we observed temperature distributions on two additional planes—z-y planes at x = 4.33 mm, and -4.33 mm.

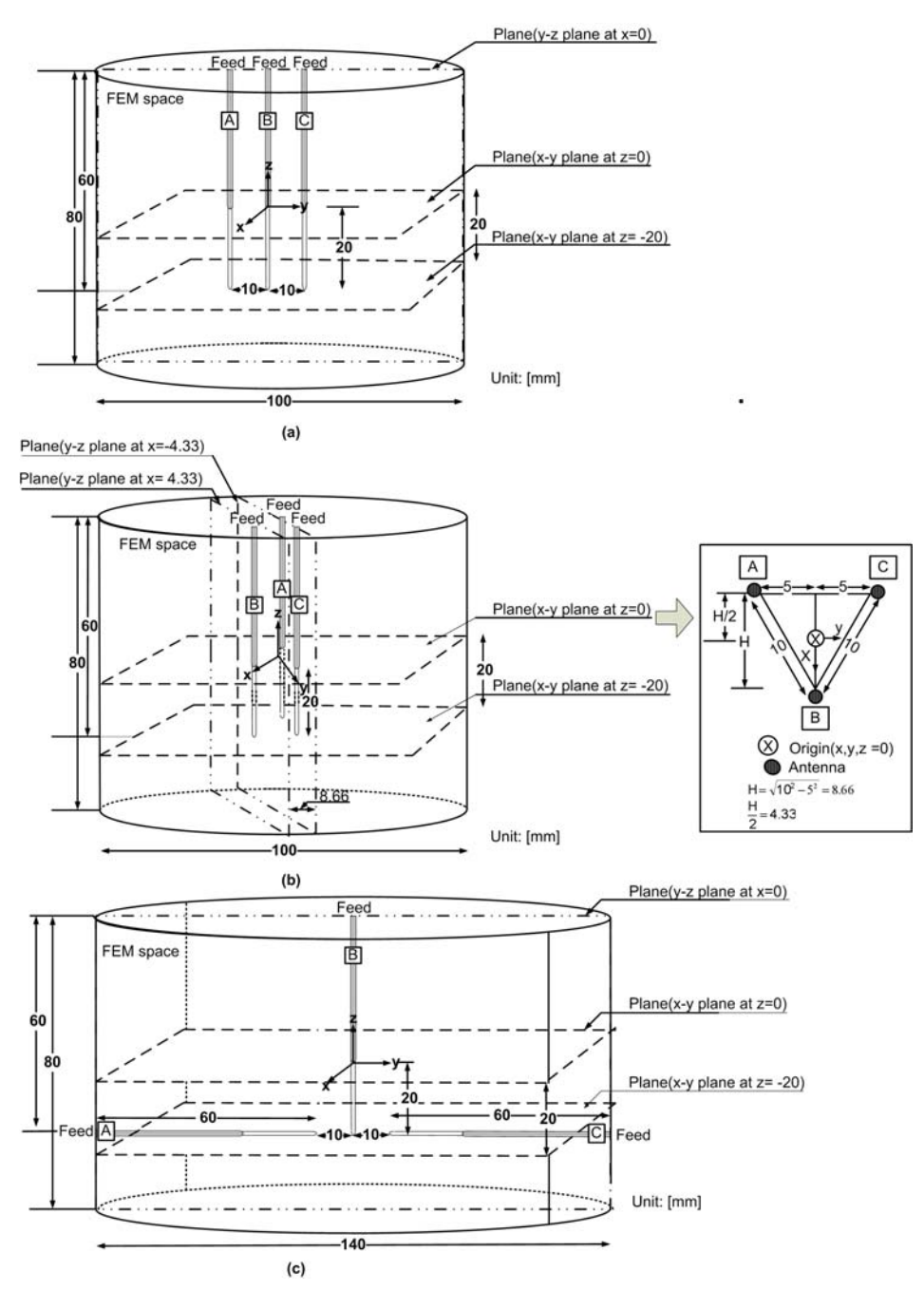


Fig. 4. Triple-antenna configurations used in this study: (a) array, (b). triangular, and (c). orthogonal arrangements.

3). Orthogonal Configuration (orthogonal): COA antennas A, B, and C, were all placed on the y-z plane (x=0) (Fig. 4 (c)). A and C were placed horizontally on the y-z plane (at z = -20 mm), parallel to the y-axis, while antenna B was placed vertically along the z-axis. A, B, and C, were arranged so that the distance between distal ends of A and B,

as well as between B and C, were 10 mm. Similar to the previous cases, the insertion depth of B was 60 mm. The overall geometry of Case 3 was also cylindrical, with 80 mm height, and 140 mm diameter. Temperature distributions on y-z plane at x = 0, and x = 0,

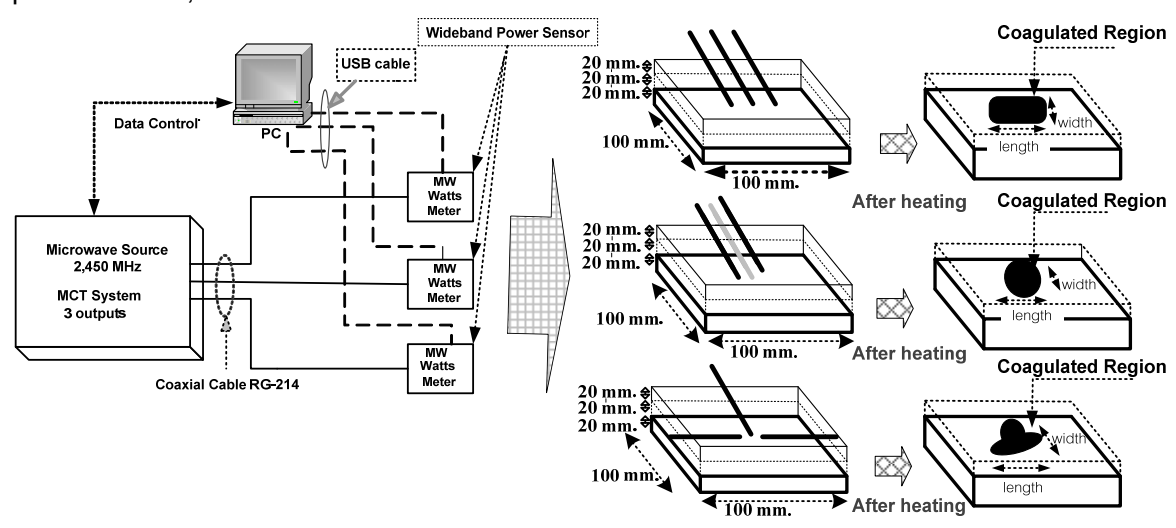


Fig. 5. Schematic diagram for *in vitro* experimental setup consisting of MW source with three outputs for different antenna arrangements. The swine liver was pre-dissected into smaller pieces in order to aide lesion dimensions measurements after MW ablation.

F. In vitro Experimental Setup

Fig. 5 shows a diagram for the experimental setup using a 3-output MW source capable of controlling the energy level of each antenna independently [15]. The MW source is a magnetron oscillator working at 2450 MHz, with maximum CW output of 250 W. The setup also consisted of three sets of measurement systems (Wideband power sensor Model 5012 (350-4000 MHz) ((Bird Electronic Corporation, Cleveland, Ohio, USA)) for delivering power to each antenna. Each sensor was linked to a PC (Pentium D 2.8 GHz, Window XP service Pack 2, 2 GB RAM, 300 GB hard disk) via USB 2.0 cable. All three MW generators were powered on simultaneously to achieve synchronous ablation.

We cut swine liver into 3 pieces in order to aide investigation of lesion formation at different locations of the tissue (Fig. 5). Each piece of liver tissue used was shaped as a rectangular prism with dimensions of 100×100×20 mm. Three configurations for antenna placement were used—array, triangular, and orthogonal, described in the previous section.

Each antenna was held at a fixed position by placing it through a narrow passage on an acrylic frame.

Similar to FE simulations, we utilized three types of antenna designs —COA, CSA, and CIA—for *in vitro* experiments. MW power of 50 W was applied to each antenna for 60 s. Before applying MW energy to the liver, we adjusted the temperature of the liver to be approximately 37 °C using a water bath heater. We also added NaCl into water to increase the conductivity to a level similar to physiological fluid (0.9% Saline). Measurements of tissue discolored areas (n=10) were recorded for comparison with FE results.

G. Triple-antennas with Mixed Designs (Mixed Antennas)

We performed triple-antenna MW ablation by arranging the antenna configurations as described in Section E. However, three different antenna designs (COA+CSA+CIA) were used simultaneously ("array mixed", "triangular mixed", and "orthogonal mixed"). Temperature distributions and lesion formations were recorded for comparison with the identical antennas cases.

TABLE 4.

VOLUMES OF LESION FORMATIONS FOR SINGLE COA, CSA, AND CIA

Single Antenna	Volume (cm ³)
COA (9.7
CSA	6.8
CIA	9.2

<u>4. ผลการทดลอง</u>

A. Comparison of COA, CSA, and CIA (Single Antenna)

We performed 3-D FE analyses of MW antenna using different single antenna designs (Fig. 1). Table 3 lists the numbers of elements used in each case, after performing Cauchy Convergence Test. When using the CIA, FE models had higher numbers of elements than those of other antenna designs because there were several thin layers of materials at the distal end of antennas. Thus, finer mesh was required in order to correctly

represent those smaller areas.

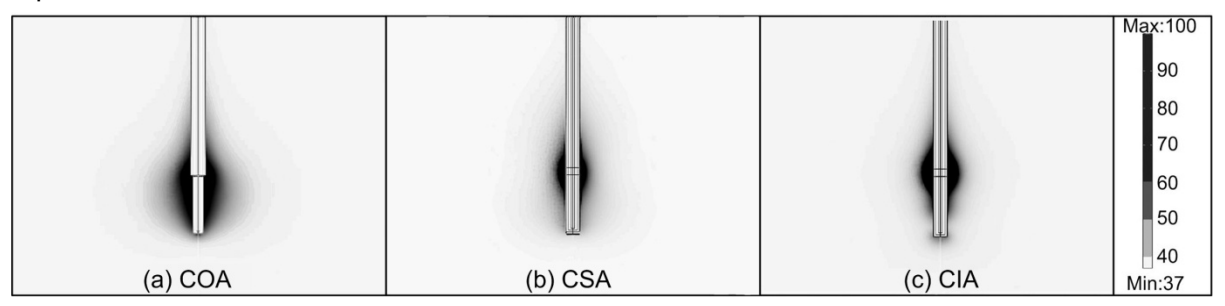


Fig. 6. Temperature distributions (50 W, 60 s) of single MW ablation from (a). COA (b). CSA, and (c). CIA. The darkest regions in each case represent areas where temperature exceeds 50 $^{\circ}$ C.

TABLE 5.

COMPARISON OF LESION CHARACTERISTICS OF "ARRAY", "TRIANGULAR", AND

"ORTHOGONAL" COA*

	Width (mm)	Length (mm)	Thickness	Volume	Computation
			(mm)	(cm ³)	Time (s)
Array COA	34	41	33	26.8	10,189
Triangular COA*	29	30	32	19.4	12,189
Orthogonal COA	45	80	31	30.2	19,313

^{*}The width and length from triangular configuration are measured on the "back" plane. The computation time required for the simulation of each case is also listed.

We applied 50 W power for a duration of 60 s in all cases. Fig. 6 (a), (b), and (c) show temperature distributions of single COA, CSA, and CIA, respectively. Regions with highest temperature were focused along the perimeter of the open tip for COA. For CSA and CIA, hot spots were located next to the slot of the antenna, with CIA having a larger area of high temperature. The destruction zone (tissue volume with temperature higher than 60 °C) can be calculated by summing the volumes of elements with temperature of 60 °C or higher. The volume of lesion formation when using COA was the largest, while the lesion formation from CSA was the smallest (Table 4). Thus, we selected COA for triple-antennas configurations in the following sections.

B. Multiple-Antenna Configurations Using COA

Since COA was the optimal single antenna design, we performed 3-D FE analyses

of triple-antenna ablation by arranging COA antennas in array, triangular, and orthogonal patterns (Fig. 4). Similar to single antenna MW ablation, we applied 50 W power for a duration of 60 s for all cases. The numbers of tetrahedral elements used in FE models are listed in Table 3.

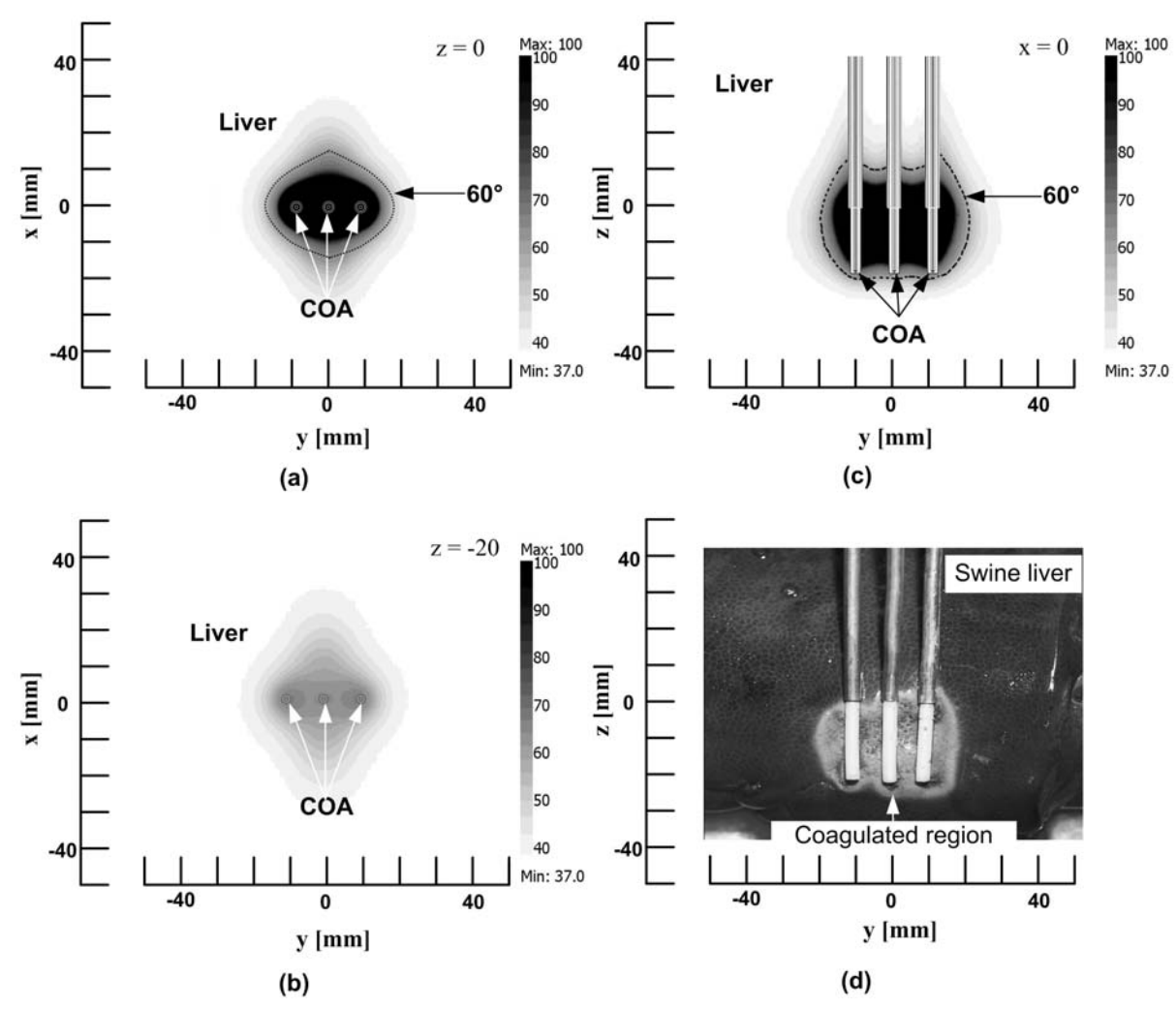


Fig. 7 Simulation and *in vitro* experimental results for array COA. (a) and (b) are temperature distribution from FE model shown on x-y plane at z = 0, and z = -20 mm, respectively. (c) is the temperature distribution on the y-z plane at x = 0 (middle of the lesion), and (d) is the corresponding *in vitro* experimental results. The dotted lines in (a) and (c) mark the extent of discolored tisuse region (Temperature exceeds 60° C).

1) Array Configuration: Fig. 7 (a) and (b) show temperature distributions of array COA on x-y plane at z = 0, and -20 mm, respectively. Fig. 7 (c) shows temperature distribution of array COA on y-z plane at x = 0 mm. The darkest regions which denote the

areas with highest temperature distribution were located around each of the three COA. The dotted line indicates areas where temperature exceeds 60 °C. From the results, the highest temperature of 90.3 °C was found at the onset of the open-tip portion of antennas A and C, on the right and left side, respectively. Table 5 lists lesion dimensions of array COA.

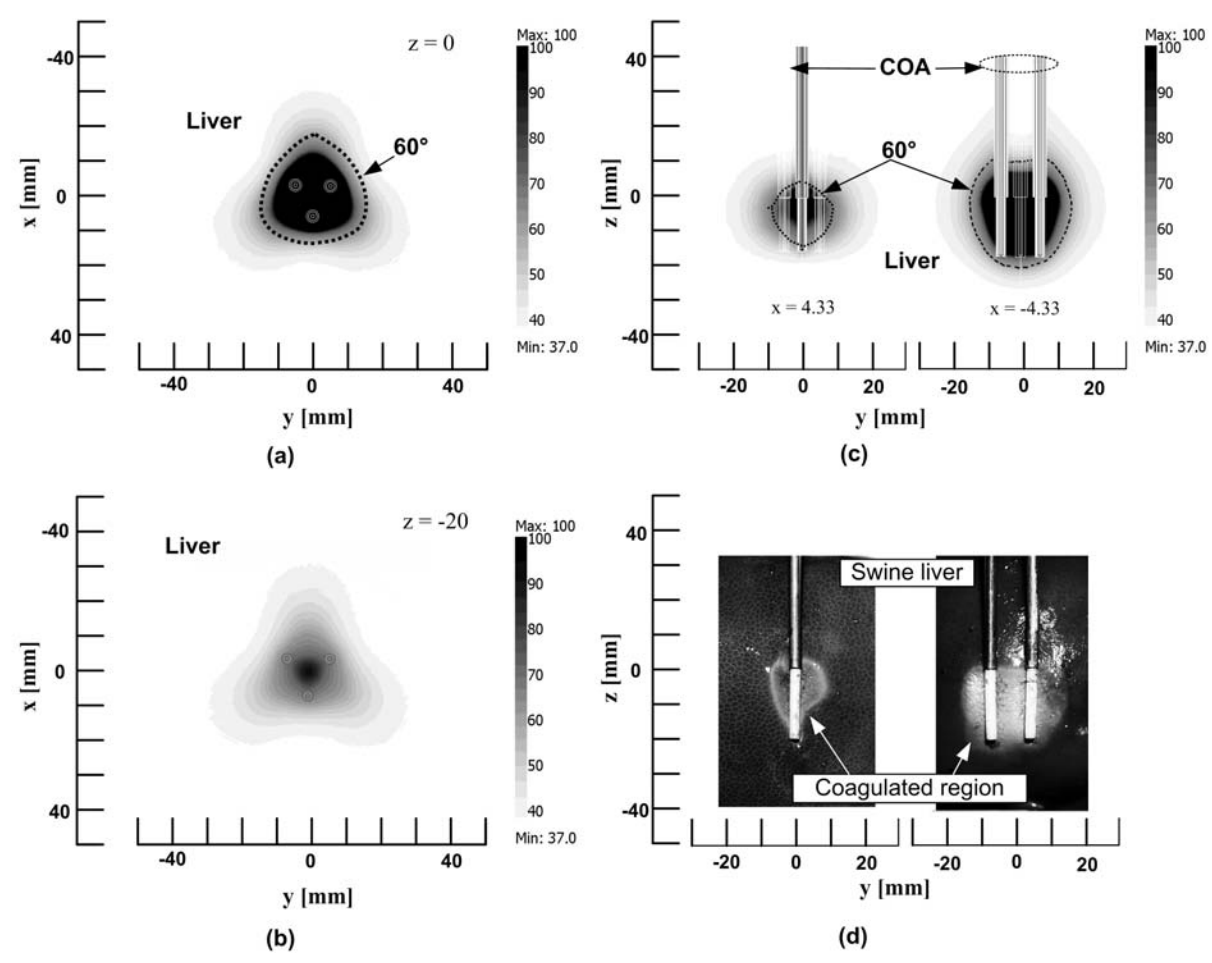


Fig. 8. Simulation and *in vitro* experimental results for triangular COA. (a) and (b) are temperature distribution from FE model shown on x-y plane at z = 0, and z = -20 mm, respectively. (c) is the temperature distribution on the y-z plane at x = 4.33 mm, and x = -4.33 mm, and (d) is the corresponding *in vitro* experimental results. The dotted lines in (a) and (c) mark the extent of discolored region

2) Triangular Configuration: Fig. 8 (a) and (b) show temperature distributions of triangular COA on x-y plane at z=0, and -20 mm, respectively. Fig. 8 (c) shows temperature distribution of triangular COA on y-z plane, at x=4.33, and -4.33 mm. The

highest temperature distributions were located around each of the three COA. From the results, highest temperature was found at (0, 0, -3.2) mm which is centrally located among the three antennas and it was equal to 98.8 $^{\circ}$ C. Table 5 lists lesion dimensions of triangular COA.

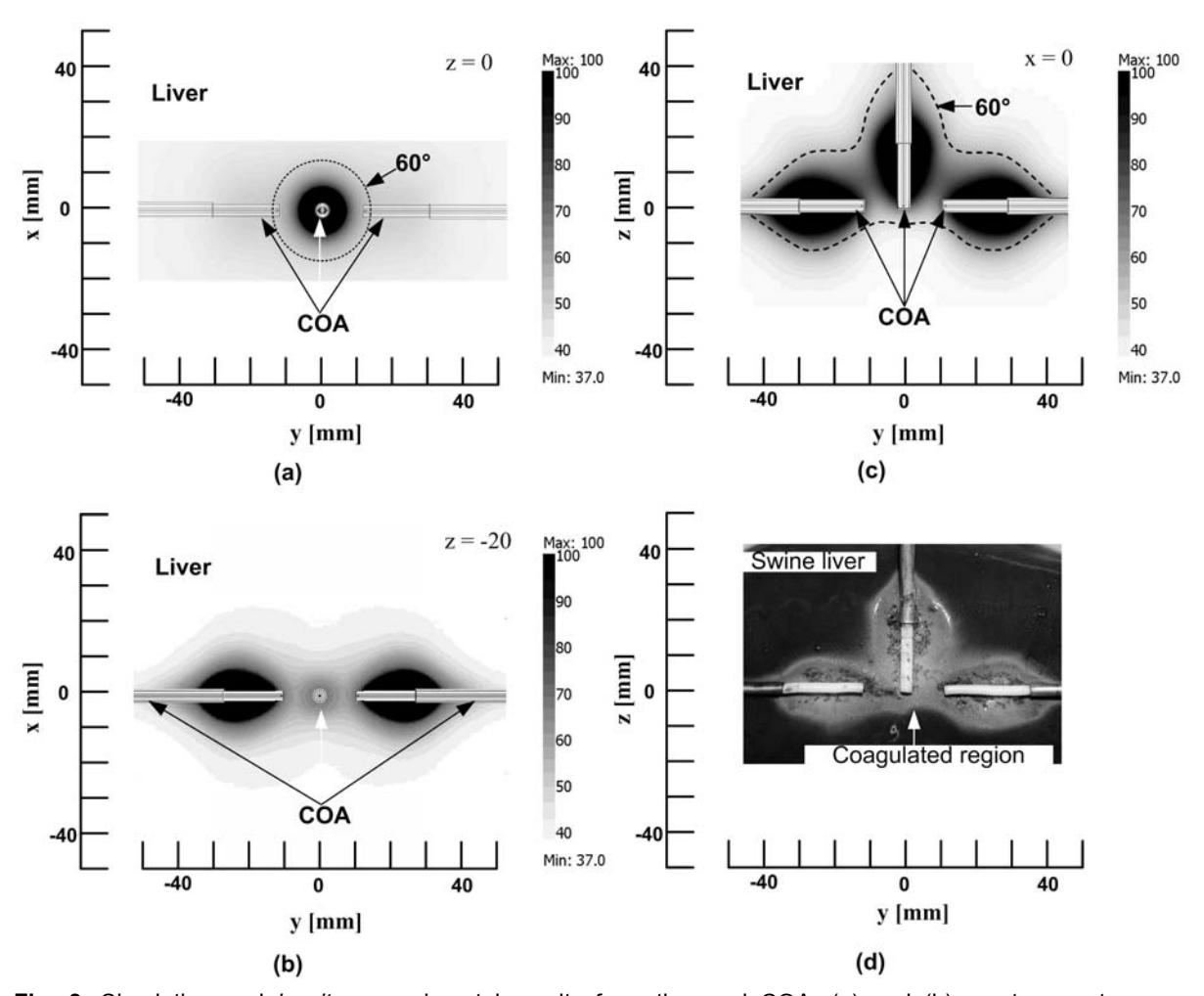


Fig. 9. Simulation and *in vitro* experimental results for orthogonal COA. (a) and (b) are temperature distribution from FE model shown on x-y plane at z = 0, and z = -20 mm, respectively. (c) is the temperature distribution on the y-z plane at x = 0 (middle of the lesion), and (d) is the corresponding *in vitro* experimental results. The dotted lines in (a) and (c) mark the extent of discolored region

3) Orthogonal Configuration: Fig. 9 (a) and (b) show temperature distributions of orthogonal COA on x-y plane at z = 0, and -20 mm, respectively. Fig. 9 (c) shows temperature distribution of orthogonal COA on y-z plane, at x =0 mm. The areas with highest temperature distribution were located adjacent to each of the three COA. From the

results, highest temperature locations were focused around the junctions at the onset of the open-tip area and it was equal to $85.2\,^{\circ}$ C. Table 5 lists lesion dimensions of orthogonal COA.

TABLE 6.
SIMULATION VS. IN VITRO EXPERIMENTAL RESULTS FOR ARRAY, TRIANGULAR,
AND ORTHOGONAL COA

Configuration		simulation		in vitro	
		Width (mm)	Length (mm)	Width (mm)	Length(mm)
Array COA		34	41	30.1±0.9	39.0±0.8
Triangular COA	Front antenna	21	20	20.1±0.7	18.2±0.8
	Back antenna	29	30	27.4±0.6	29.4±0.9
Orthogonal COA		45	80	43.7±0.8	79.1±0.7

C. Comparison of Results from FE Analyses and in vitro Experiments

We performed *in vitro* experiments as described in Section III D using the same conditions as our FE models in the previous sections. As we dissected the tissue at the planes of interest prior to MW ablation, tissue discoloration areas were photographed with a digital camera (Nikon D70s, Nikon Corp., Tokyo, Japan) for all cases. Fig. 7 (d), 8 (d), and 9 (d) illustrate that *in vitro* lesion characteristics from array, triangular, and orthogonal triple COA antennas are comparable to FE results in Fig. 7 (c), 8 (c), and 9 (c). Lesion widths and lengths from FE models and *in vitro* experiments are listed in Table 6.

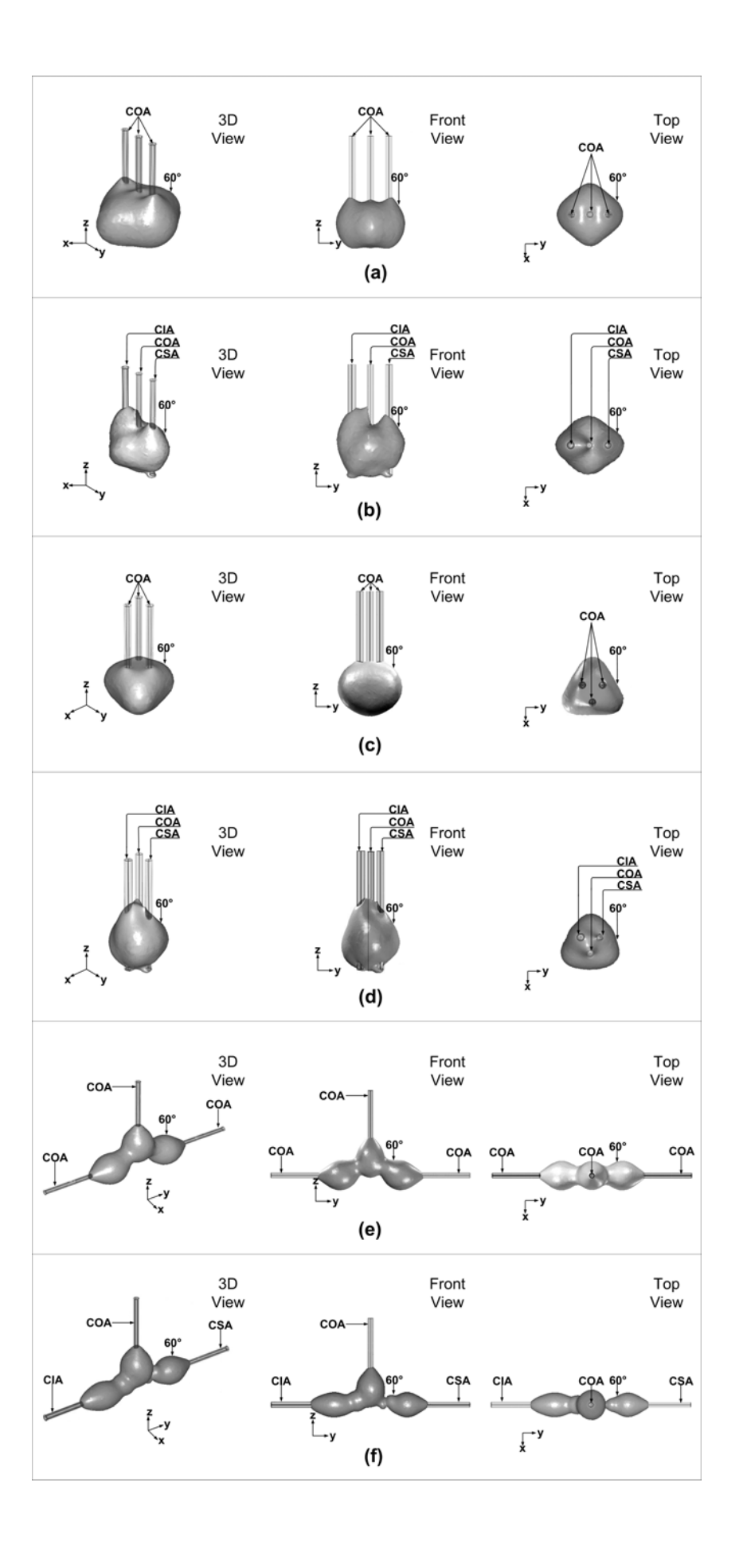


Fig. 10. Three-dimensional representations of lesions formed when triple COA and triple mixed antennas were used. (a) and (b) are lesion formations for array configuration of triple COA, and triple mixed antennas; (c) and (d) are lesion formations for triangular configuration of triple COA, and triple mixed antennas; and (e) and (f) are lesion formations for orthogonal arrangment of triple COA, and triple mixed antennas.

D. Mixed Designs for Triple-Antenna MW Ablation

To compare the differences in geometrical characteristics of identical triple-antenna MW ablation versus those of mixed triple ablation MW ablation, we illustrated the resulted lesion formations in 3-D in Fig. 10 (a) to Fig. 10 (f). The 3-D geometries of lesion formations for array COA, triangular COA, and orthogonal COA are shown in Fig. 10 (a), 10 (c), and 10 (e), respectively, while those for "array mixed", "triangular mixed", and "orthogonal mixed", are shown in Fig. 10 (b), 10 (e), and 10 (f), respectively.

Lesion formation for array COA appears to be symmetric from the top view, while lesion formation around CIA appears to be larger than that close to CSA for mixed array. Similarly, lesion characteristics for triangular and orthogonal COA exhibit some symmetry, while it is evident from Fig. 10 (d) and Fig. 10 (f) that "triangular mixed" and "orthogonal mixed" MW ablation resulted in asymmetric lesions and more lesion formation was found close to CIA, compared to CSA.

5. วิจารณ์ผลการทดลอง

For single MW antenna ablation, COA was able to create the largest lesion volume. When comparing VSWR of the three antenna designs (Fig. 2), CIA has the best matching impedance at frequency of 2.45 GHz—that is, its VSWR is closest to perfect matching (VSWR = 1.0). Matching impedance of CSA is slightly better than that of COA. However, lesion volume for COA was the largest because MW energy was able to propagate into larger tissue area adjacent to the open-tip. MW energy propagation for CSA and CIA was limited to a smaller area surrounding the slot, thus CSA and CIA had smaller lesion formation. In addition, lesion volume of CIA was larger than CSA due to a better impedance matching (Fig. 2).

For identical triple-antenna ablation, orthogonal configuration has the largest lesion volume, followed by lesion volumes of array and triangular configurations, respectively.

However, in real application, orthogonal arrangement is more difficult to place inside a patient's body. For triangular pattern, lesion characteristics were similar to using a single antenna, but the resulted lesion volume was twice as large.

Resulted lesion dimensions from FE simulations are slightly larger than those of the *in vitro* experiments, but otherwise exhibit a similar trend, with orthogonal configuration having the largest lesion dimensions, and the triangular configuration having the smallest lesion. The discrepancies in lesion dimensions between FE analyses and *in vitro* experiments range from 1.1 to 12.9%. Thus, we conclude that our FE analyses offer satisfying results in this study as FE model was able to accurately predict lesion characteristics of different triple-antenna MW ablations.

The resulted lesion volumes from using mixed designs triple-antennas were generally smaller than those of three COA triple-antennas, independent of antennas configuration. In addition to lesion volumes, a major difference in the results of the two cases was lesion characteristics. Lesions formed when we used COA triple-antenna exhibited a certain degree of symmetry—opposite y-z plane for array configuration, around z-axis for triangular configuration, and y-z plane for orthogonal configuration. In contrast, lesions formed when we used mixed antenna designs were asymmetric, and the destruction zone adjacent to CIA appeared to be larger than that of CSA. This is highly evident in the case of orthogonal configuration (Fig. 10 (e) and (f)). In addition, comparison of our results with previous studies also showed that, for a similar targeted lesion volume, triple-antenna ablation requires shorter duration than double-antenna ablation [20].

<u>6. สรุป</u>

In this study, we utilized 3-D FE analyses for single- and triple-antenna hepatic MW ablation. Three designs for single-antenna MW ablation were compared and COA was found to produce largest lesions, compared to those from CSA, and CIA. Although single-antenna can destroy a reasonable amount of cancer tissue, larger lesions are often required for more advanced stage of cancer. Thus, triple-antenna ablation can potentially be employed to produce large lesions as well as more varied lesion characteristics. Three triple-antenna configurations—"array", "triangular", and "orthogonal"—were investigated using FE analyses and validated with *in vitro* experiments in this study. In addition to using identical antennas for triple-antenna hepatic MW ablation, we also employed three distinct

antenna designs simultaneously (mixed antennas). As expected, triple-antenna MW ablation produced larger lesion formation than that of single-antenna MW ablation. Using identical antennas for triple-antenna MW ablation provides generally symmetric lesion formation, while using non-identical antennas produced non-symmetric lesions. In practice, we can employ non-identical triple-antenna to destroy cancer tissue of varied geometrical shapes. For example, when cancer tissue is adjacent to a large blood vessel where cooling effect from blood withdraws some thermal energy from MW ablation, we can focus MW energy towards that area without overheating normal tissue located further away from the blood by using appropriate non-identical multi-antenna ablation.

7. ข้อเสนอแนะสำหรับงานวิจัยในอนาคต

For future studies, I plan to modify the three-source MW ablation generator as the overall size of the system is large (approximately 1 mm x 80 mm x 80 mm). A new system is under development and will be markedly smaller thus making the MW generator much more mobile. I plan to collaborate with medical doctors at various hospitals in Bangkok as well as in Madison, Wisconsin, USA for possible in vivo experiments in animal lab and eventually for use in human subjects. The FE modeling technique that I have developed can also be used to simulate additional new antenna designs. In addition, this technique can also be applied for other diseases such as prostate cancer, and lung cancer.

หนังสืออ้างอิง

- [1] <u>T. L. Fong</u>, "Liver cancer online document", [Online]. Available: http://www.medicinenet.com/liver_cancer/article.htm
- [2] T. J. Vogl, T. K. Helmberger, M. G. Mack, and M. F. Reiser (Eds.), "Ablative techniques (percutaneous) The ermal Ablative Techniques," in *Percutaneous Tumor Ablation in Medical Radiology*, Berlin, Germany: Springer, 2008, pp. 7–32.
- [3] J. P. McGahan, J. M. Brock, H. Tesluk, W.-Z. Gu, P. Schneider, and P. D. Browing, "Hepatic ablation with use of radio-frequency electrocautery in the animal model," *J. Vasc. Inter. Radiol.*, vol. 3, pp. 291–297, 1992.
- [4] B. Chiappini, R. Di Bartolomeo, and G. Marinelli, "The surgical treatment of atrial fibrillation with microwave ablation: preliminary experience and results," *Interactive Cardiovascular and Thoracic Surgery*. [Online]. 2(2003), pp. 327–330. Available: http://icvts.ctsnetjournals.org/cgi/content/full/2/3/327
- [5] D. M. Mahvi, "Radiofrequency ablation of hepatic malignancies: Is heat better than cold?," *Ann. Surg.*, vol. 230, no. 1, pp. 9–11, 1999.
- [6] A. S. Wright, D. M. Mahvi, D. G. Haemmerich, and F. T. Lee, "Minimally invasive approaches in management of hepatic tumors," *Surg. Tech. International XI.*, pp. 144—153, 2003.
- [7] D. Haemmerich, F. T. Lee, JR., "Multiple applicator approaches for radiofrequency and microwave ablation," *Int. Journal. Hyperthermia.*, vol. 21, no. 2, pp. 93–106, Mar. 2005.
- [8] M. W. Miller and M. C. Ziskin, "Biological consequences of hyperthermia," Ultrasound Med. Biol., vol. 15, pp. 707–722, 1989.
- [9] S. A. Sapareto and W. C. Dewey, "Thermal dose determination in cancer therapy," Int. J. Radiation Oncol. Biol. Phys., vol. 10, pp. 787–800, 1984.
- [10] Organ LW, "Electrophysiologic principles of radiofrequency lesion making," *Appl Neurophysiol.*, vol. 39, no. 2, pp. 69–76, 1976.
- [11] C. Cha, F. T. Lee, Jr., L. F. Rikkers, J. E. Niederhuber, B. T. Nguyen, D. M. Mahvi, "Rationale for the combination of cryoablation with surgical resection of hepatic tumors," *Journal of Gastrointestinal Surgery*, vol. 5, no. 2, pp.206—213, 2001.
- [12] S. B. Chinn, F. T. Lee, Jr., G. D. Kennedy, C. Chinn, C. D. Johnson, T. C. Winter III, T. F. Warner, and D. M. Mahvi, "Effect of vascular occlusion on radiofrequency ablation

- of the liver: results in a porcine model," *AJR Am J Roentgenol.*, pp.789–795, Mar. 2001.
- [13] A. S. Wright, L. A. Sampson, T. F. Warner, D. M. Mahvi, and F. T. Lee, "Radiofrequency versus microwave ablation in a hepatic Porcine Model," *Radiology*., vol. 236, pp. 132—139, 2005.
- [14] F. T. Lee, D. Haemmerich, A. S. Wright, D. M. Mahvi, L. A. Sampson, and J. G. Webster, "Multiple probe radiofrequency ablation: pilot study in an animal model," J Vasc Interv Radiol., vol. 14, pp. 1437—1442, 2003.
- [15] F. Burdío, A Güemes, J. M. Burdío, A. Navarro, R. Sousa, T. Castiella, I. Cruz, O. Burzaco, X. Guirao, and R. Lozana, "Large hepatic ablation with bipolar saline-enhanced radiofrequency: an experimental study in *in vivo* porcine liver with a novel approach," *Journal of Surgical Research.*, vol. 110, no. 1, pp. 193–201, Mar. 2003.
- [16] M. Kuang, M. D. Lu, X. Y. Xie, H. X. Xu, L. Q. Mo, G. J. Liu, Z. F. Xu, Y. L. Zheng, and J. Y. Liang, "Liver cancer: increased microwave delivery to ablation zone with cooled-shaft antenna—experiment and clinical studies," *Radiology.*, vol. 242, no. 3, pp. 914–924, Mar. 2007.
- [17] D. Haemmerich, F. T. Lee, D. J. Schutt, L. A. Sampson, J. G. Webster, J. P. Fine, and D. M. Mahvi, "Large-volume radiofrequency ablation of ex vivo bovine liver with multiple cooled cluster electrodes," *Radiology*., vol. 234, no. 2, pp. 563–568, Feb. 2005.
- [18] M. Lu, J. Chen, X. Xie, L. Liu, X. Huang, L. Liang, and J. Huang, "Hepatocellular carcinoma: US-guided percutaneous microwave coagulation therapy," *Radiology*., vol. 221, no. 1, pp. 167–172, Oct. 2001.
- [19] S. Labonté, A. Blais, S. R. Legault, H. O. Ali, and L. Roy, "Monopole antennas for microwave catheter ablation," *IEEE Trans. Microw. Theory Tech.*, vol. 44, no. 10, pp. 1832—1840, Oct. 1996.
- [20] K. Saito, Y. Hayashi, H. Yoshimura, and K. Ito, "Heating characteristics of array applicator composed of two coaxial-slot antennas for microwave coagulation therapy," IEEE Trans. Microw. Theory Tech., vol. 48, no. 11, pp. 1800—1806, Nov. 2000.

- [21] A. S. Wright, F. T. Lee, Jr., and D. M. Mahvi, "Hepatic microwave ablation with multiple antennae results in synergistically larger zones of coagulation necrosis," *Annals of Surgical Oncology*., vol. 10, no. 3, pp. 275–283, 2003.
- [22] S. A. Shock, K. Meredith, T. F. Warner, L. A. Sampson, A. S. Wright, T. C. Winter III, D. M. Mahvi, J. P. Fine, and F. T. Lee, "Microwave ablation with loop antenna: *in vivo* porcine liver model," *Radiology.*, vol. 231, no. 1, pp. 143—149, Apr. 2004.
- [23] J. C. Lin, and Y.-J. Wang, "The cap-choke catheter antenna for microwave ablation treatment," *IEEE Trans. Biomed. Eng.*, vol. 43, no. 6, pp. 657—660, Jun. 1996.
- [24] D. Yang, J. M. Bertram, M. C. Converse, A. P. O'Rourke, J. G. Webster, S. C. Hagness, J. A. Will, and D. M. Mahvi, "A floating sleeve antenna yields localized hepatic microwave ablation," *IEEE Trans. Biomed. Eng.*, vol. 53, no. 3, pp. 533—537, Mar. 2006.
- [25] D. Panescu, J. G. Whayne, S. D. Fleischman, M. S. Mirotznik, D. K. Swanson, and J. G. Webster, "Three-dimensional finite element analysis of current density and temperature distributions during radio-frequency ablation," *IEEE Trans. Biomed. Eng.*, vol. 42, no. 9, pp. 879—890, Sep. 1995.
- [26] S. Tungjitkusolmun, E. J. Woo, H. Cao, J. Z. Tsai, V. R. Vorperian, and J. G. Webster, "Finite element analyses of uniform current density electrodes for radio-frequency cardiac ablation," *IEEE Trans. Biomed. Eng.*, vol. 47, no. 1, pp. 32—40, Jan. 2000.
- [27] E. J. Woo, S. Tungjitkusolmun, H. Cao, J. Z. Tsai, J. G. Webster, V. R. Vorperian, and J. A. Will, "A new catheter design using needle electrode for subendocardial RF ablation of ventricular muscles: Finite element analysis and *in vitro* experiments," *IEEE Trans. Biomed. Eng.*, vol. 47, no. 1, pp. 23—31, Jan. 2000.
- [28] E. J. Berjano, and F. Hornero, "Thermal-electrical modeling for epicardial atrial radiofrequency ablation," *IEEE Trans. Biomed. Eng.*, vol. 51, no. 8, pp. 1348—1357, Aug. 2004.
- [29] D. Haemmerich, S. Tungjitkusolmun, S. T. Staelin, F. T. Lee, Jr., D. M. Mahvi, and J. G. Webster, "Finite-element analysis of hepatic multiple probe radio-frequency ablation," *IEEE Trans. Biomed. Eng.*, vol. 49, no. 7, pp. 836–842, Jul. 2002.

- [30] D. Haemmerich, S. T. Staelin, S. Tungjitkusolmun, F. T. Lee, D. M. Mahvi, and J. G. Webster, "Hepatic bipolar radio-frequency ablation between separated multiprong electrodes," *IEEE Trans. Biomed. Eng.*, vol. 48, no. 10, pp. 1145—1152, Oct. 2001.
- [31] K. M. Jones, J. A. Mechling, J. W. Strohbehn, and B. S. Trembly, "Theoretical and experimental SAR distributions for interstitial dipole antenna arrays used in hyperthermia," *IEEE Trans. Microwave Theory Tech.*, vol. 37, no. 8, pp. 1200—1209, Aug. 1989.
- [32] S. Pisa, M. Cavagnaro, P. Bernardi, and J. C. Lin, "A 915-MHz antenna for microwave thermal ablation treatment: Physical design, computer modeling and experimental measurement," *IEEE Trans. Biomed. Eng.*, vol. 48, no. 5, pp. 599—601, May. 2001.
- [33] G. Schaller, J. Erb, R. Engelbrecht, and H. M. Seegenschmiedt, "Field simulation of applicators for interstitial microwave hyperthermia," *IEEE MTT-S Digest.*, vol. 4, pp. 307—310, 1995.
- [34] G. Schaller, J. Erb, and R. Engelbrecht, "Field simulation of dipole antennas for interstitial microwave hyperthermia," *IEEE Trans. Microw. Theory Tech.*, vol. 44, no. 6, pp. 887—895, Jun. 1996.
- [35] W. Hürter, F. Reinbold, and W. J. Lorenz, "A dipole antenna for interstitial microwave hyperthermia," *IEEE Trans. Microw. Theory Tech.*, vol. 39, no. 6, pp. 1048–1054, Jun. 1991.
- [36] J. C. Lin, S. Hirai, C.-L. Chiang, W.-L. Hsu, J.-L. Su, and Y.-J. Wang, "Computer simulation and experimental studies of SAR distributions of interstitial arrays of sleeved-slot microwave antennas for hyperthermia treatment of brain tumors," *IEEE Trans. Microw. Theory Tech.*, vol. 48, no. 11, pp. 2191—2198, Nov. 2000.
- [37] K. Saito, T. Taniguchi, H. Yoshimura, and K. Ito, "Estimation of SAR distribution of a tip-split array applicator for microwave coagulation therapy using the finite element method," *IEICE Trans. Electronics.*, vol. E84–C, no. 7, pp. 948–954, Jul. 2001.
- [38] H. H. Pennes, "Analysis of tissue and arterial blood temperatures in the resting human forearm," *J Appl Phy.*, vol. I, pp. 93—122, Aug. 1948.

Output จากโครงการวิจัยที่ได้รับทุนจาก สกว.

1. ผลงานตีพิมพ์ในวารสารวิชาการนานาชาติ หรือนำเสนอในการประชุมวิชาการ นานาชาติ

- 1.1 S. Tungjitkusolmun, M. Chaichanyut, P. Lertprasert, M. Krairiksh, "Finite Element Method for Analyses of Magnetic and Electric Field Distribution of Monopole Antennas in Liver Tissue," 2004 IEEE International Workshop on Biomedical Circuits & Systems, December 1-3, 2004, Singapore.
- 1.2 S. Tungjitkusolmun, A. Boontaram, P. Lertprasert, M. Krairiksh, "Finite Element Analyses for a study of hepatic cancer tissue destruction using monopole and bipolar radio-frequency ablation," 3rd IASTED International Conference on Biomedical Engineering (BIOMED 2005), February 16-18, 2005, Innsbruck, Austria
- 1.3 P. Phasukkit, M. Sangworasil, S. Tungjitkusolmun, "Estimation of SAR and temperature distribution from microwave ablation technique using 2-D axisymmetric finite element analysis," International Conference on Engineering, Applied Sciences, and Technology (ICEAST 2007), November 21-23, 2007
- 1.4 P. Phasukkit, K. Yencham, A. Chaiyapong, S. Tansawat, C. Buakaew, M. Sangworasil, and S. Tungjitkusolmun, "3-D Finite element for microwave coagulation therapy for liver and lung cancer using triple-antennas technique," International Conference on Engineering, Applied Sciences, and Technology (ICEAST 2007), November 21-23, 2007
- 1.5 Z. Sun, T. Chaichana, Y. Allen, M. Sangworasil, S. Tungjitkusolmun, D. E. Hartley, and M. M. Lawrence-Brown, "Investigation of hemodynamic changes in abdominal aortic aneurysms, treated with fenestrated endovascular grafts," 13th Interational Conference on Biomedical Engineering (ICBME 2008), December 3-6, 2008, Singapore 1.6 Z. Sun, T. Chaichana, M. Sangworasil, and S. Tungjitkusolmun, "Computational fluid analysis of blood flow characteristics in abdominal aortic aneurysms treated with suprarenal endovascular grafts," 13th Interational Conference on Biomedical Engineering (ICBME 2008), December 3-6, 2008, Singapore
- 1.7 Z. Sun, T. Chaichana, T. Nipawan, M. Sangworasil, S. Tungjitkusolmun, J. Chaorensuk, N. Phoocharoen, Y. B. Allen, D. E. Hartley, M. M. Lawrence-Brown,

"Simulation of blood flow in abdominal aortic aneurysms pre- and post-fenestrated stent graft repair: A preliminary study, Int. J. CARS (2008), 3 (Suppl 1): S64-S67

1.8 Pattarapong Phasukkit, Manas Sangworasil, and Supan Tungjitkusolmun, "Analysis of placement configurations of triple antenna microwave ablation," submitted to IEEE Trans. Biomedical Engineering, 2009.

2. การนำผลงานวิจัยไปใช้ประโยชน์

-เชิงสาธารณะ

- ได้ร่วมงานลาดกระบังนิทรรศ์ เดือน พฤศจิกายน 2549
- ให้สัมภาษณ์สารคดีทางด้านงานวิจัยวิทยาศาสตร์ สถานีโทรทัศน์ข่อง 9 อสมท
- ให้สัมภาษณ์นำเสนองานวิจัยในรายการเที่ยงวันทันข่าว สถานีโทรทัศน์ช่อง 3
- ให้สัมภาษณ์หนังสือพิมพ์ Post Today ตามเอกสารแนบในภาคผนวก

-เชิงวิชาการ

- เป็นหัวข้อวิจัยสำหรับนักศึกษาปริญญาโท และ เอก ที่ภาควิชาอิเล็กทรอนิกส์ คณะ วิศวกรรมศาสตร์ สถาบันเทคโนโลยีพระจอมเกล้าเจ้าคุณทหารลาดกระบัง
- จัดอบรม workshop การใช้โปรแกรมไฟในต์เอลิเมนต์สำหรับงานวิจัยทางวิศวกรรม
- ได้ใช้ความเชี่ยวชาญทางการวิเคราะห์ไฟในต์เอลิเมนต์ไปใช้ในงานวิจัยที่เกี่ยวข้อง คือ การศึกษาการไหลของเลือดในหลอดเลือดที่มีปัญหา และได้ตีพิมพ์บทความวิจัยตามที่ ได้แนบไว้ในภาคผนวก

3. อื่น ๆ

-